Interaction of uranium from seepage water with hydroxyapatite

Jens Mibus, Vinzenz Brendler

1 Forschungszentrum Rossendorf, Institute of Radiochemistry, P.O. Box 51 01 19, D-01314 Dresden, Germany, E-mail: J.Mibus@fz-rossendorf.de

Abstract. Column experiments (in a quartz matrix) assisted by batch experiments helped to quantify and characterize the uranium(VI) retardation by hydroxyapatite, regarded as a highly efficient component of reactive barrier concepts for (radio)toxic contaminants. The sorption of uranyl ions onto phosphate groups is as important as their sorption onto silanol groups, outweighing the low phosphate content. In column experiments retardation factors ranging around 30 were observed. The elution of uranium is governed by two processes of different rate (and probably reversibility) which is consistent with the spectroscopic findings.

Introduction

The protection of the biosphere from hazards due to the release of radionuclides from abandoned uranium mining and processing as well as from final repositories for nuclear waste continues to be a challenge for scientists and engineers. A system of engineered and geological barriers is foreseen to ensure the isolation of pollutants potentially released from the waste.

A number of substances, such as clay minerals, zeolites, or phosphates, have the ability to scavenge metal ions from aqueous solutions. Thus, they are potential materials for the construction of barrier systems or can be used as additional for a retardation or even permanent immobilization of toxic or radiotoxic metals.

Hydroxyapatite HAP ($Ca_{10}(PO_4)_6(OH)_2$) is known for its strong interaction with lanthanides and actinides (Jerden and Sinha 2003). Whereas rare earth elements (REE) are proven to substitute calcium in the crystal lattice of HAP (Jones et al. 1996), actinides are supposed to form surface complexes or surface precipitates. Several uranyl phosphate minerals are stable under weathering conditions.

Well-understood basic processes and a reliable database are essential prerequisites for any assessment modeling of the retardation efficiency of reactive barriers. Here, the major goals are: a) the identification of the species involved in surface

reactions of uranium with HAP under oxidizing conditions, and b) the characterization of these processes and the investigation of their reversibility. Both targets are so far not addressed in the literature. The work described below is embedded into a larger project also involving batch experiments with uranium(VI) and pure mineral phases (HAP, quartz, gibbsite, kaolinite, illite, and montmorillonite) as well as surface complexation modeling of these systems linked to independent spectroscopic proofs of the respective surface species.

Materials and Methods

Materials

A commercially available synthetic hydroxyapatite p.a. (Merck, Germany) was used for all experiments. A mean grain size of 15 µm was certified by the manufacturer. BET measurements (a five-point N_2-BET Coulter SA 3100) yielded a specific surface area of 65.3 m²/g. The chemical composition of the solid was verified by ICP-MS (ELAN 5000-ICP-MS, Perkin Elmer), indicating only very minor amounts of impurities: 510 ppm Si, 200 ppm Al, 180 ppm Fe, 73 ppm Mn, and 26 ppm Ti. A marine quartz sand from Heerlen, Netherlands (supplier Euroquartz, Dorsten, Germany) was applied as matrix material in the column experiments (mean grain size 150 µm, $Fe_2O_3 \leq 0.01$ %, $Al_2O_3 \leq 0.05$ %, $TiO_2 \leq 0.02$ %). The quartz sand was washed with MilliQ water to remove soluble constituents. We used a seepage water synthesized in the laboratory according to original samples from a rock pile of the former uranium mining (shaft 66) in Schlema (Germany) reported in Geipel et al. (1994). The composition is given in Table 1. All experiments were carried out under atmospheric conditions at room temperature.

Table 1. Composition of the synthetic seepage water.

Ion	Concentration [mmol/L]
Ca^{2+}	7.8
Mg^{2+}	17.1
Na^{+}	0.5
UO_2^{2+}	0.01[a]
SO_4^{2-}	25.6
PO_4^{3-}	< 0.02
HCO_3^{-}	0.45
Cl^{-}	0.1
pH	7.82

[a] Solutions for conditioning purposes in the batch and column experiments were prepared without uranium (tracer-free solution).

Batch experiments

A quantity of 0.5 g HAP was placed in a 50 mL polypropylene vial. Subsequently, 40 mL of the tracer-free seepage water were added. After conditioning for four weeks and pH equilibration, 0.4 mL of a 10^{-3} M $UO_2(NO_3)_2$ solution were injected to reach the tracer concentration given in Table 1. After a contact time of 64 hours the samples were centrifuged and the uranium content in the supernatant was measured. Finally, the adsorption to the vial walls was measured and the results were corrected accordingly.

Column experiments

A laboratory column (1.0 m length and 0.1 m diameter) was tightly packed with quartz sand containing 0.1 % by weight HAP. Micro suction probes (Rhizon SMS, Eijkelkamp, Netherlands) were installed at distances of 0.1, 0.3, 0.5, 0.7, and 0.9 m from the inlet.

The column was percolated with seepage water at a constant Darcy velocity of $(9.5 \pm 0.5) \cdot 10^{-8}$ m/s. The solution was injected at the top and drained at the bottom of the column. Thus, variable water saturated conditions were reached. After conditioning with tracer-free solution for six months (phase 1) seepage water containing 10^{-5} M U(VI) was applied for eight months yielding a long rectangular pulse injection (phase 2). After that the column was rinsed with tracer-free seepage water for twelve months (phase 3). All suction probes and the column outlet were sampled weekly and analyzed for pH, major ions, and uranium. The transport parameters of a conservative tracer were measured by means of tritiated water under the same flow conditions.

After 610 days (370 days after starting phase 3) solid material was taken from sealable openings at the positions of the suction probes. Aliquots of 2 g were used to determine the volumetric water content. The material was washed with MilliQ water to remove the pore solution probably disturbing spectroscopic measurements.

Spectroscopic investigations

The uranium speciation influenced by various processes such as aqueous complexation, surface complexation, surface precipitation or formation of secondary phases was investigated applying advanced spectroscopic tools. Two series of samples were analyzed. Five solid samples were taken after 610 days from the column and treated as described above. Immediately before that also five aqueous samples were extracted. Time-resolved laser-induced fluorescence spectroscopy (TRLFS) was applied due to its high sensitivity for uranium and the provision of three independent information blocks: the intensity of the fluorescence emission, the spectral shift, and the decay time of the fluorescence signal (describing the time after which the signal has decreased to *1/e* of the start intensity), allowing in

combination a distinction of a variety of uranium surface species and dissolved complexes coupled with semi-quantitative results.

The TRLFS system consists of a Nd:YAG diode laser with subsequent fourth harmonic generation. This wavelength (266 nm) was used for the excitation of the samples, providing an optimal signal-to-noise ratio. The emitted fluorescence radiation was focussed into a spectrograph and the resulting spectra were measured by a diode array (701 intensified diodes). The gate width (exposure time) is variable from 5 ns to 2 ms. Here, 5 µs were used. The delay time after the excitation laser pulse ranges from 0 ns to 6500 ns. For further details concerning the set-up of the TRLFS equipment and operation modes see Geipel et al. (1996). Every spectrum was measured three times, and for each spectrum 100 laser shots were averaged. 31 spectra at steadily increasing delay times were collected totally for one time-resolved spectrum.

Results

Aqueous speciation of uranium(VI)

There are extensive reviews of the aqueous uranium speciation available, the most prominent work was performed under the auspices of the Nuclear Energy Agency (NEA) within the Organisation for Economic Co-operation and Development (OECD). As part of the NEA Thermochemical Database a special volume dedicated to uranium was issued in 1992 (Grenthe et al., 1992), with major revisions published in 2003 (Guillaumont et al., 2003). Based on these data and applying the EQ3/6 geochemical speciation code (Wolery, 1992) the aqueous speciation of uranium in the pH range of interest between 7 and 9 was computed. It turned out that the neutral aqueous complex $Ca_2UO_2(CO_3)_3$ (Bernhard et al., 2001) is the dominating species under the applied experimental conditions, binding around 78 % of all uranium at pH 7 and rising up to nearly 100 % at pH 7.5 and higher. Between pH 7 and 7.5 the contribution from the ternary aqueous complex $(UO_2)_2CO_3(OH)_3^-$ decreases from about 15 % to zero. The calculations furthermore did not indicate any supersaturation with respect to possible secondary uranium phases. Namely, the amount of silica and phosphate released by quartz and HAP dissolution processes, respectively, was too low to precipitate uranyl silicate or uranyl phosphate minerals. Even the formation of respective aqueous uranyl complexes can be neglected.

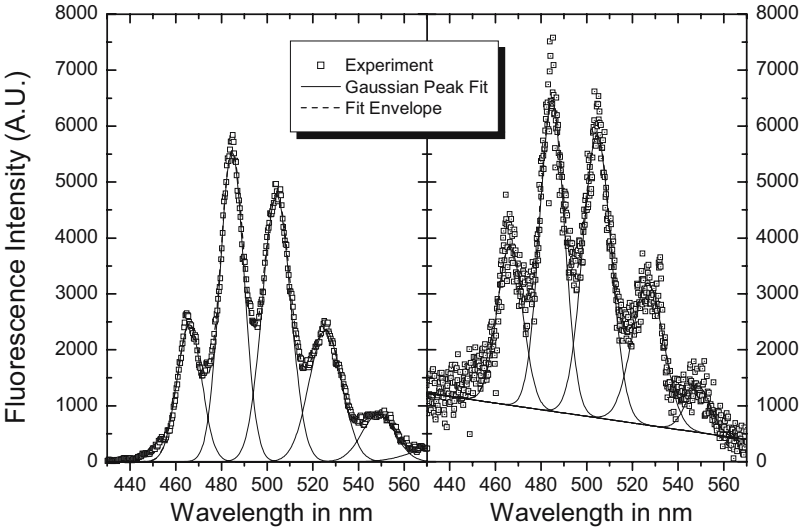

Fig. 1. Fluorescence spectra with peak deconvolution of $Ca_2UO_2(CO_3)_3(aq)$ (left side) and pore water from the quartz/HAP column (right side).

These predictions were compared with the spectroscopic findings. A typical spectrum of the aqueous samples is shown on the right side of Fig. 1. The spectrum on the left side was obtained from a solution containing just the neutral $Ca_2UO_2(CO_3)_3$ uranium species. A comparison of the two spectra show a similar blue shift of the major five peaks, of about –5 nm with respect to the uncomplexed uranyl ion in acidic solutions (Bell and Biggers, 1968; Brachmann, 1997). In addi-

Table 2. Fluorescence properties of selected aqueous uranium species.

Spectroscopic Characteristics	Free UO_2^{2+} [a]	$Ca_2UO_2(CO_3)_3$ [b]	This work
1st Peak in nm	472	466	466.4
2nd Peak in nm	488	484	484.9
3rd Peak in nm	510	504	504.5
4th Peak in nm	535	524	526.8
5th Peak in nm	560	-	548.8
Lifetime in ns	1570	43	50

[a] Brachmann, 1997, [b] Bernhard et al., 2001

tion, the fluorescence decay times (43 ns for the $Ca_2UO_2(CO_3)_3$ complex and about 50 ns for the column samples) are very similar. Therefore it is very likely that indeed (as postulated by the geochemical computations) the neutral $Ca_2UO_2(CO_3)_3$ complex is dominating the aqueous uranium speciation. The spectroscopic properties are summarized in Table 2.

Sorption of uranium(VI) onto HAP

In the batch experiments a strong interaction of the uranium contained in the seepage water with HAP was observed. The measured equilibrium concentrations of uranium in the supernatant amounts to $(2.7 \pm 0.3) \cdot 10^{-9}$ M, *i.e.*, four orders of magnitude lower than in the starting solution. Uranium adsorbs nearly quantitatively to the HAP surface. The calculation of the distribution coefficient K_D from this equilibrium concentrations is not meaningful for the steep slope of K_D at adsorption rates approaching 100 %.

The surface speciation of uranium on apatite-like minerals has been investigated in several works: Drot et al., 1998; Fuller et al., 1996 & 2002; Arey et al., 1999; Simon et al., 2004. Unfortunately, no parameter sets for surface complexation models have been derived so far for this system, thus prohibiting predictive modeling.

In addition, the small amount of HAP compared to quartz results in rendering uranyl quartz surface species strong competitors to any uranyl reactions onto phosphate surface groups. This holds despite the much weaker character of the silanol uranyl bond when compared to the phosphate uranyl bond.

Again, the TRLFS investigation proved to be a valuable tool to discriminate between the various possible surface complexes. The measured spectra are rather small and noisy but nevertheless a proper data processing reveals the major spectroscopic properties. The fluorescence decay indicated two distinctive species having lifetimes of (569 ± 53) ns and of (54.6 ± 0.6) µs. However, their major fluorescence peaks did not differ significantly. The peak maxima occur at 482.8, 502.0, 522.1, 547.0, 571.1, and 599.5 nm. This corresponds to an average shift of +11 nm relative to the free uranyl cation. A comparison with typical spectra obtained from uranium sorbed onto pure HAP (average wavelength shift of +12 nm and lifetimes of 570 ns and 3.5 µs) and pure quartz (average wavelength shift of +9 nm and lifetimes of 780 ns and 45 µs) showed that the uranium surface species with the shorter lifetime clearly can be attributed to uranyl sorbed onto HAP. The uranium surface species with the longer lifetime probably is a uranyl unit bond to a silanol surface group from quartz.

Transport behavior of uranium

The interpretation of the tracer transport in the porous medium is based on the one-dimensional transport equation

$$R_f \frac{\partial c}{\partial t} = D \frac{\partial^2 c}{\partial x^2} - v \frac{\partial c}{\partial x} \quad (1)$$

where c is the tracer concentration, v is the pore-water velocity, D is the hydrodynamic dispersion coefficient, R_f is the retardation factor, t is the time, and x is the distance. R_f is related to the empirical distribution coefficient K_D by

$$R_f = 1 + \frac{\varsigma K_D}{\theta} \quad (2)$$

where ς represents the dry bulk density and θ the volumetric water content of the porous medium. The connection between pore-water velocity and Darcy velocity v_D is given by

$$v = \frac{v_D}{\theta} \quad (3).$$

The according parameters were estimated using the CXTFIT code (Toride et al. 1995).

The volumetric water content θ in the column determined gravimetrically at the observed vertical positions is given in Table 3. Water unsaturated conditions occur in the upper three positions whereas the transition zone to water saturated condi-

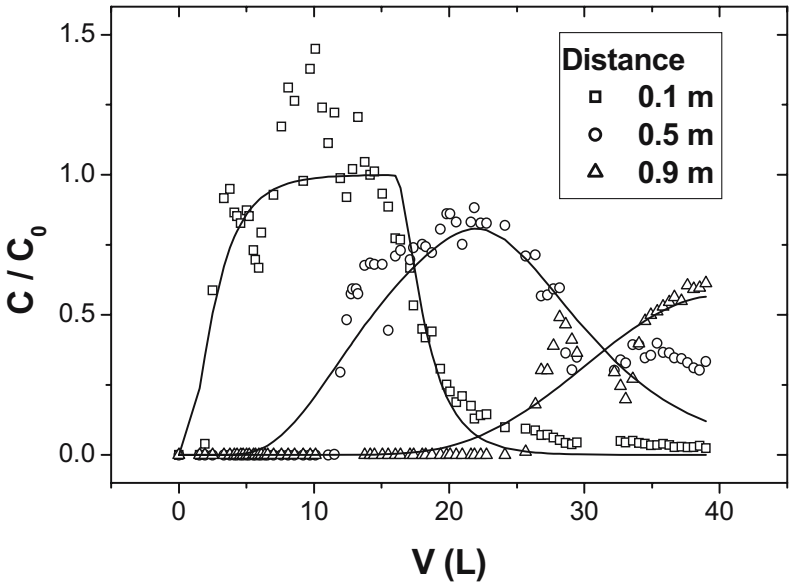

Fig. 2. Breakthrough curves of uranium normalized to the input concentration C_0 vs. eluted volume at different distances from the inlet (symbols: experimental values, lines: model).

tions is located in the bottom part.

The breakthrough curves (BTC) of uranium normalized to the input concentration C_0 and the corresponding model curves are depicted in Fig. 2. The fitted parameters v, D, and R_f are shown in Table 3. The BTC's exhibit a steeply rising edge. The subsequent expected plateau in phase two is overlaid by concentrations exceeding C_0 in the first monitored position (x = 0.1 m). This could be produced by a temporarily increased input concentration, ion exchange processes displacing uranium, or a mobilization of colloid borne uranium. So far, the reason is not clear. The maximum concentration at the different vertical positions continuously decreases over the column length. The dropping edge of the uranium BTC's exhibits a long tailing at a low concentration level ($0.02 \cdot C_0$ at x = 0.1 m) which was not observed to that degree in the tritium BTC's. Therefore, a double porosity effect in the unsaturated zone might play a role, however, the tailing of the uranium curves is clearly influenced kinetically.

Certainly, the simple model based on the K_D concept is not able to describe the breakthrough behavior perfectly. Above all it fails to model the kinetic processes, *i.e.*, the long tailing. The derived R_f values can only describe the arrival of the contaminant plume, but not its elution. The R_f values over the column length show only minor differences. In the transition zone to the saturated zone it is slightly increased and drops in the saturated zone. In general the observed heterogeneity of the transport properties is small at this scale.

Evaluating the BTC at x = 0.1 m it becomes clear that the elution of uranium is governed by two processes. A fast desorption results in a swift dropdown followed by a slow release over a long period which is not yet completed. This is in concordance with the residual uranium concentration in the solid at the uppermost position where elution is in progress. It still amounts to about 30 % of the solid concentration at the lower positions. Since the elution proceeds at a low level we cannot prove the full irreversibility of the fixation of uranium. The calculation of a recovery makes no sense unless the BTC dropped to zero. Nevertheless, the slow release yields in low uranium concentrations of approximately 10^{-7} mol/L.

Table 3. Transport parameters derived from the column experiment.

Distance	θ^a	$v^{b,c}$	$D^{b,c}$	$R_f{}^b$	$C_{solid}{}^d$
[m]	[mL/mL]	[10^{-6} m/s]	[10^{-8} m^2/s]	[-]	[mg/kg]
0.1	0.09±0.005	1.00±0.05	2.1±0.1	32±3	1.4±0.1
0.3	0.09±0.005	0.97±0.05	0.5±0.03	38±4	3.4±0.3
0.5	0.08±0.005	0.98±0.05	1.0±0.05	37±4	5.3±0.5
0.7	0.13±0.006	0.98±0.05	1.1±0.05	45±4	3.9±0.4
0.9	0.46±0.02	0.53±0.03	0.4±0.02	27±3	3.7±0.4

[a] determined gravimetrically; [b] fitted parameters from CXTFIT; [c] determined from tritium BTC; [d] U concentration in the solid after 610 days

Conclusions

Time-resolved laser-induced fluorescence spectroscopy proved to be a valuable tool in supporting column sorption experiments. We were thus able to identify relevant uranium(VI) species both in solution and on surfaces. Sorption is a significant process and dominated by silanol and phosphate groups stemming from quartz and HAP, respectively. The specific binding (chemisorption) of uranium onto phosphate surface binding sites is much stronger than to silanol groups. This occurrence of two surface species corresponds to the findings from the column experiments. It seems logical to assign the faster sorption / desorption scheme to the uranyl silanol surface species, exhibiting an almost full reversibility. The second observed process creating the long and pronounced tailing in the BTC's can be explained by the much stronger binding of the uranyl moiety to the phosphate sites. There, the significantly lower reversibility may also arise from a beginning surface precipitation or diffusion of UO_2^{2+} into the crystal lattice. This, however, has still to be proven by further spectroscopic investigations. Furthermore, the transport model has to be extended by kinetic terms and appropriate parameters in order to enable a profound prediction of the long-term behavior.

In general, the addition of phosphate mineral such as HAP even at low concentrations will efficiently increase the retardation. It must, however, be kept in mind that HAP is stable only at pH above 5 (depending on the background concentration of calcium), thus other retarding additives are required for reactive barriers designed to operate also under acidic conditions. The next step is to investigate the influence of the background electrolyte composition, namely with high concentration of other cations competing with the uranyl cation for sorption sites.

Acknowledgement

The authors gratefully acknowledge experimental support, assistance in data processing and fruitful discussions with many colleagues from the Institute of Radiochemistry, especially Gerhard Geipel, Nils Baumann, Susanne Sachs, Sina Brockmann, and Christa Müller.

References

Arey JS, Seaman JC, Bertsch PM (1999) Immobilization of uranium in contaminated sediments by hydroxyapatite addition. Environ. Sci. Technol. 33: 337-342

Bell JT, Biggers RE (1968) Absorption spectrum of the uranyl ion in perchlorate media III. Resolution of the ultraviolet band structure: Some conclusions concerning the excited state of UO_2^{2+}. J. Mol. Spectrosc. 25: 312-329

Bernhard G, Geipel G, Reich T, Brendler V, Amayri S, Nitsche H (2001) Uranyl(VI) carbonate complex formation: Validation of the $Ca_2UO_2(CO_3)_3$(aq.) species. Radiochim. Acta 89: 511-518

Brachmann A (1997) *Zeitaufgelöste laser-induzierte Fluoreszenzspektroskopie zur Charakterisierung der Wechselwirkung des Uranylions mit Huminsäuren und Carboxylatliganden.* Ph.D. Thesis. TU Dresden, 198pp

Drot R, Simoni E, Alnot M, Ehrhardt JJ (1998) Structural environment of uranium(VI) and europium(III) species sorbed onto phosphate surfaces: XPS and optical spectroscopy studies. J. Coll. Interf. Sci. 205: 410-416

Fuller CC, Bargar JR, Davis JA, Piana MJ (2002) Mechanisms of uranium interactions with hydroxyapatite: implications for groundwater remediation. Environ. Sci. Technol. 36: 158-165

Fuller CC, Davis JA, Coston JA, Dixon E (1996) Characterization of metal adsorption variability in a sand gravel aquifer, Cape Cod, Massachusetts, U.S.A. J. Contam. Hydrol. 22: 165-187

Geipel G, Brachmann A, Brendler B, Bernhard G, Nitsche H (1996) Uranium(VI) sulfate complexation studied by time-resolved laser-induced fluorescence spectroscopy (TRLFS). Radiochim. Acta 75: 199-204

Geipel G, Thieme M, Bernhard G, Nitsche H (1994) Distribution of uranium and radionuclides in a uranium-mining rockpile in Schlema, Saxony, Germany. Radiochim. Acta 66/67: 305-308

Grenthe I, Fuger J, Lemire RJ, Muller AB, Nguyen-Trung C, Wanner H (1992) *Chemical Thermodynamics of Uranium*. Elsevier, Amsterdam

Guillaumont R, Fanghänel T, Fuger J, Grenthe I, Neck V, Palmer DA, Rand MH (2003) *Update on the chemical thermodynamics of uranium, neptunium, plutonium, americium and technetium*. Chemical Thermodynamics Vol. 5 (OECD Nuclear Energy Agency, ed.), Elsevier, Amsterdam

Jerden JL jr., Sinha AK (2003) Phosphate based immobilization of uranium in an oxidizing bedrock aquifer. Appl. Geochem. 18: 823-843.

Jones A, Wall F, Williams C (1996) Rare earth minerals: chemistry, origin and ore deposits. Chapman Hall, London, 372p.

Simon FG, Biermann V, Segebade C, Hedrich M (2004) Behaviour of uranium in hydroxyapatite-bearing permeable reactive barriers: investigation using ^{237}U as a radioindicator. Sci. Total Environ. 326: 249-256

Toride N, Leji FJ, van Genuchten MT (1995) *The CXTFIT Code for Estimating Transport Parameters from Laboratory or Field Tracer Experiments. Version 2.1*. Research Report No. 137. U.S. Salinity Laboratory, Agricultural Research Service, U.S. Department of Agriculture, Riverside, California

Wolery TJ (1992) *EQ3/6, A software package for the geochemical modeling of aqueous systems.* UCRL-MA-110662 Part I, Lawrence Livermore National Laboratory